0026-895X/99/040658-10$3.00/0

MOLECULAR PHARMACOLOGY, **55:**658–667 (1999).

Pyrrolidine Dithiocarbamate Prevents I-κB Degradation and Reduces Microvascular Injury Induced by Lipopolysaccharide in Multiple Organs

SHU FANG LIU,[1] XIAOBING YE,[1] and ASRAR B. MALIK

Department of Pharmacology, The University of Illinois, College of Medicine, Chicago, Illinois

Received August 12, 1998; accepted December 15, 1998

This paper is available online at http://www.molpharm.org

ABSTRACT

Lipopolysaccharide (LPS) is a key mediator of multiple organ injury observed in septic shock. The mechanisms responsible for LPS-induced multiple organ injury remain obscure. In the present study, we tested the hypothesis that the LPS-induced injury occurs through activation of the transcription factor, nuclear factor-κB (NF-κB). We examined the effects of inhibiting NF-κB activation in vivo in the rat on LPS-induced: 1) gene and protein expression of the cytokine-inducible neutrophil chemoattractant (CINC) and intercellular adhesion molecule-1 (ICAM-1); b) neutrophil influx into lungs, heart, and liver; and c) increase in microvascular permeability induced by LPS in these organs. LPS (8 mg/kg, i.v.) challenge of rats activated NF-κB and induced CINC and ICAM-1 mRNA and protein expression. Pretreatment of rats with pyrrolidine dithiocarbamate (50, 100, and 200 mg/kg, i.p.), an inhibitor of NF-κB activation, prevented LPS-induced I-κBα degradation and the resultant NF-κB activation and inhibited, in a dose-related manner, the LPS-induced CINC and ICAM-1 mRNA and protein expression. Pyrrolidine dithiocarbamate also markedly reduced the LPS-induced tissue myeloperoxidase activity (an indicator of tissue neutrophil retention) and the LPS-induced increase in microvascular permeability in these organs. These results demonstrate that NF-κB activation is an important in vivo mechanism mediating LPS-induced CINC and ICAM-1 expression, as well as neutrophil recruitment, and the subsequent organ injury. Thus, inhibition of NF-κB activation may be an important strategy for the treatment of sepsis-induced multiple organ injury.

Multiple organ injury, a frequent complication of sepsis, is characterized by microvascular injury and increased vascular endothelial permeability (Brigham et al., 1979; Fowler et al., 1985; Meyrick et al., 1986). One crucial event that leads to microvascular endothelial damage and multiple organ injury is endothelial "activation" and neutrophil infiltration and accumulation in various organs (Brigham et al., 1979; Meyrick et al., 1986; Bone, 1991; Parrillo, 1995; Ward, 1996). Bacterial endotoxin (lipopolysaccharide, LPS) initiates this pathophysiological process through multiple but cooperative pathways. LPS induces the expression of adhesion molecules [E-selectin, P-selectin, and intercellular adhesion molecule-1 (ICAM-1)] on endothelial cells, which mediate neutrophil margination, rolling, and firm adhesion (Carlos and Harlan, 1994). LPS also activates and up-regulates integrins (CD11b/CD18) on the neutrophil cell surface (Carlos and Harlan, 1994). Interactions between ICAM-1 and CD11b/CD18 lead to neutrophil adhesion to the endothelium (Carlos and Harlan, 1994), followed by neutrophil activation, change in neutrophil shape, and migration through the endothelial cell junctions into surrounding tissue (Carlos and Harlan, 1994). Activated neutrophils release oxidant free radicals and proteinases, resulting in endothelial damage (Tate and Repine, 1983; Weiss, 1989). LPS also causes the expression of chemokines including interleukin (IL)-8, macrophage inflammatory proteins (MIPs), and cytokine-induced neutrophil chemoattractant (CINC) in several constitutive cells and resident macrophages (Ben-Baruch et al., 1995; Frevert et al., 1995; Koh et al., 1995; Blackwell et al., 1996; Ward, 1996). Release of these chemokines as well as leukotriene B4 and complement C5 within the interstitium sets up a chemoattractant gradient for neutrophil migration into tissue (Ward, 1996; Mulligan et al., 1996). LPS also releases other proinflammatory cytokines, which can amplify the inflammatory response and mediate tissue damage (Bone, 1991; Parrillo, 1995). The

This work was supported by National Heart, Lung, and Blood Institute Grants HL46350 (to A.B.M.) and the American Heart Association Grant-in-Aid 9650733N (to S.F.L.).

[1] Current address: Division of Pulmonary & Critical Care Medicine, Albert Einstein College of Medicine, New Hyde Park, New York.

ABBREVIATIONS: EMSA, electrophoretic mobility shift assay; GAPDH, glyceraldehyde phosphate dehydrogenase; PDTC, pyrrolidine dithiocarbamate; NF-κB, nuclear factor-κB; AP, activating protein; ICAM-1, intercellular adhesion molecule-1; CINC, cytokine-inducible neutrophil chemoattractant; MPO, myeloperoxidase; MIP, macrophage inflammatory protein; TNF-α, tumor necrosis factor-α; IL, interleukin; DTT, dithiothreitol; PMSF, phenylmethylsulfonyl fluoride.

sequential events and cooperative interactions of adhesion molecules and chemokines mediating LPS-induced inflammation suggest that common molecular mechanisms such as activation of the transcription factor nuclear factor-κB (NF-κB) may be important in orchestrating the response.

Deletion mutagenesis of the promoters and reporter gene analysis in cultured cells, primarily in cell lines, has shown that NF-κB plays an essential role in the transcriptional induction of cell adhesion molecules ICAM-1, E-selectin, and vascular adhesion molecule-1) and chemokines (IL-8, CINC, MIP-1, and MIP-2) (Baeuerle and Henkel, 1994; Carlos and Harlan, 1994; Siebenlist et al., 1994; Collins et al., 1995). NF-κB is also involved in LPS-induced expression of proinflammatory cytokines and enzymes that contribute to endothelial damage and development of multiorgan injury (Baeuerle and Henkel, 1994; Siebenlist et al., 1994). Because NF-κB activation may be crucial in the LPS-induced multiple organ injury, in the present study, we studied the effects of inhibiting NF-κB activation using pyrrolidine dithiocarbamate (PDTC) on LPS-induced: 1) CINC and ICAM-1 mRNA and protein expression; 2) neutrophil infiltration; and 3) increase in microvascular permeability in multiple organs. Our data indicate that NF-κB activation is an important in vivo signal orchestrating the LPS-initiated adhesion and chemokine expression, neutrophil sequestration, and the resultant multiple organ injury.

Materials and Methods

Animal Protocols. Male Sprague-Dawley rats were purchased from Charles River, divided into experimental groups in a randomized manner, and used for experiments when their body weights were in the 300- to 350-g range. We studied six groups of animals: control, saline (1 ml/kg, i.v.); LPS, *Salmonella enteritidis* LPS (8 mg/kg in saline, i.v.); LPS plus PDTC groups, 50, 100, or 200 mg/kg of PDTC (i.p.) 1 h before LPS challenge; and PDTC alone, PDTC (200 mg/kg, i.p.) for an equivalent period of time. All procedures were approved by the Institutional Animal Care Committee.

Animals were sacrificed by exsanguination, and lung, heart, and liver were collected either at 1 h [for electrophoretic mobility shift assay (EMSA)] or at 4 h post-LPS challenge [for Northern, Western blot, and enzyme-linked immunosorbance assay (ELISA)]. Animals in the PDTC alone group were sacrificed at 2 h (for EMSA) or at 5 h (for Northern, Western blot, and ELISA), and tissues were collected. Tissues were snap-frozen in liquid nitrogen and kept at −70°C for later use.

Nuclear Protein Extract and EMSA. Lungs and hearts were minced on ice in 0.5 ml ice-cold buffer A composed of: 10 mM HEPES (pH 7.9), 1.5 mM KCl, 10 mM $MgCl_2$, 0.5 mM dithiothreitol (DTT), 0.1% IGEPAL CA-630, and 0.5 mM phenylmethylsulfonyl fluoride (PMSF) (all from Sigma Chemical Co., St. Louis, MO). The minced tissue was homogenized using Dounce homogenizer, followed by centrifuging at 5000*g* at 4°C for 10 min. The crude nuclear pellet was suspended in 200 μl of buffer B (20 mM HEPES, pH 7.9, 25% glycerol, 1.5 mM $MgCl_2$, 420 mM NaCl, 0.5 mM DTT, 0.2 mM EDTA, 0.5 mM PMSF, and 4 μM leupeptidin) and incubated on ice for 30 min. The suspension was centrifuged at 16,000*g* at 4°C for 30 min. The supernatant (nuclear proteins) was collected and kept at −70°C for use. Protein concentration was determined using bicinchoninic acid assay kit with BSA as standard (Pierce, Rockford, IL).

NF-κB consensus oligonucleotide probe (5′-AGTTGAGGGGACTTTCCCAGGC-3) was end-labeled with [γ-^{32}P] ATP (Amersham Life Science, Arlington Heights, IL). Nuclear protein (10 or 20 μg for lung or heart) was incubated with 100,000 cpm ^{32}P-labeled NF-κB consensus oligonucleotide for 30 min in a total volume of 15 μl in a binding buffer that consisted of 10 mM Tris-Cl, pH 7.5, 1 mM $MgCl_2$, 50 mM NaCl, 0.5 mM DTT, 0.5 mM EDTA, 4% glycerol, and 2 μg of poly-(deoxyinosinic·deoxycytidylic acid) (Pharmacia Biotech, Piscataway, NJ). The specificity of the DNA/protein binding was determined by competition reactions in which 50-fold molar excess of unlabeled NF-κB oligonucleotide was added to the binding reaction 10 min before the addition of radiolabeled probe. Reaction was stopped by adding 1 μl of gel loading buffer and subjected to nondenaturing 4% polyacrylamide gel electrophoresis in 0.25× TBE buffer (Tris-borate-EDTA). Gel was vacuum-dried and exposed to X-ray film (Fuji hyperfilm).

Northern Blot Analysis. Rat cDNA probes for CINC (207 bp) and ICAM-1 (384 bp) were amplified using standard reverse transcription-polymerase chain reaction procedure. RNA (1 μg) from LPS-treated rat lungs was reverse transcribed into cDNA. The cDNA probe fragments were amplified from reverse transcriptase-generated cDNAs using designed primers corresponding to the published rat CINC (Huang et al., 1992) and rat ICAM-1 (Kita et al., 1992) cDNA sequences, purified by gel electrophoresis, and eluted from the gels using a Jetsorb DNA extraction kit (Genomed, Inc., Research Triangle Park, NC). Authenticity of the PCR product was confirmed by dideoxy chain termination sequencing.

Lung and heart were granulated and homogenized. Total RNA was extracted following the method described by Chomczynski and Sacchi (1987). Poly-$(A)^+$ mRNA was isolated using a poly-(A) mRNA isolation kit (Promega Corp., Madison, WI). Approximately 3 μg of mRNA from each sample were separated on a 1.2% denaturing agarose gel and transferred onto Hybond-N nylon filter (Amersham Life Science). The filter was incubated at 42°C for at least 4 h in a prehybridization buffer that consisted of 50% formamide, 5× Denhardt's solution, 5× SSC, 200 μg/ml of sonicated denatured salmon sperm DNA, and 0.1% SDS. The filter was then hybridized with 1×10^6 cpm/ml ^{32}P-labeled rat CINC, ICAM-1, and glyceraldehyde phosphate dehydrogenase (GAPDH; Fort et al., 1985) probes at 42°C for 14–16 h and washed sequentially with decreasing concentrations of SSC/0.1% SDS and at increasing temperatures (final wash, 0.1× SSC/0.1% SDS at 60°C). The blots were exposed to Fuji film in the presence of an intensifying screen for 1 to 3 days. Each hybridization was followed by film exposure and stripping down of previous probe before the subsequent hybridization to other probes.

Protein Extraction and Western Blot Analysis. Lungs, heart, and liver were finely minced and homogenized in 10 volumes of ice-cold protein extracting buffer containing 25 mM Tris-HCl, 0.5 mM EDTA, 0.5 mM EGTA, 0.1 mg/ml PMSF, 10 μg/ml of leupeptin, and 1 μM pepstain. The homogenate was centrifuged at 17,500*g* at 4°C for 15 min, and the resulting supernatant was collected as cytosolic fraction. The pellet was resuspended in extracting buffer containing 0.1% Triton X-100, homogenized, and centrifuged at 17,500*g* at 4°C again for 30 min. The second supernatant was collected and centrifuged at 90,000*g* at 4°C for 60 min. The resulting pellet was dissolved in extracting buffer and taken as membrane fraction. Protein concentration was determined using bicinchoninic acid assay kit with BSA as standard (Pierce, Rockford, IL).

Equal amounts of proteins (30 μg/lane) were loaded and separated on 7.5% (for ICAM-1), 12.5% (for I-κB), or 15% (for CINC) SDS-polyacrylamide slab gel under denaturing conditions. Broad range protein molecular weight marker (Bio-Rad, Hercules, CA) was used as standard. Proteins were electroblotted to nitrocellulose membrane (Bio-Rad). After incubation in blocking solution [5% dry milk in TBST (Tris buffered saline with Tween 20)] at room temperature for 2 h, the membrane was immunoblotted to the following antibodies at room temperature for 1 h in separate experiments: anti-I-κB monoclonal antibody (Santa Cruz Biotechnology, Santa Cruz, CA); anti-CINC polyclonal antibody (kindly provided by Dr. Zagorski at National Institutes of Health, Bestheda, MD); and anti-rat ICAM-1 monoclonal antibody (PharMingen, San Diego, CA). The secondary antibodies were horseradish peroxidase-conjugated monkey anti-goat and goat anti-mouse antibodies. Peroxidase labeling was de-

tected with enhanced chemiluminescence Western blotting detection system (Amersham Life Science) according to the manufacturer's recommendations.

Tissue CINC and ICAM-1 Content Quantification. Tissue CINC content was quantitated using sandwich ELISA as described previously (Wittwer et al., 1993). Ten μg of lung or 20 μg of heart cytosolic protein were added into each microplate well. The coating antibody was affinity-purified goat anti-CINC polyclonal antibody (kindly provided by Dr. Zagorski). The detecting antibody was polyclonal rabbit anti-CINC antibody (Peptide International, Louisville, KY) and horseradish peroxidase conjugated anti-rabbit IgG (Amersham Life Science). To determine tissue ICAM-1 level, 1 μg of lung or 5 μg of liver or heart membrane protein in 50 mM carbonate/bicarbonate buffer (pH 9.5) were added to microtitration plates (Dynatech, Chantily, VA) overnight at 4°C. The contents of the wells were removed, and wells were washed for four times with PBS containing 0.05% Tween 20 (PBST). The coated wells were blocked with 5% dry milk in PBST at room temperature for 2 h, followed by incubation with anti-rat ICAM-1 monoclonal antibody in 5% dry milk/PBST at room temperature for an additional 2 h. After washing with PBST four times, horseradish peroxidase-conjugated anti-mouse IgG in PBST was added. Color was developed by the addition of TMB peroxidase substrate mixture (Sigma Chemical Co.) and read in a microplate reader at the wavelength of 450 nm after addition of stopping buffer.

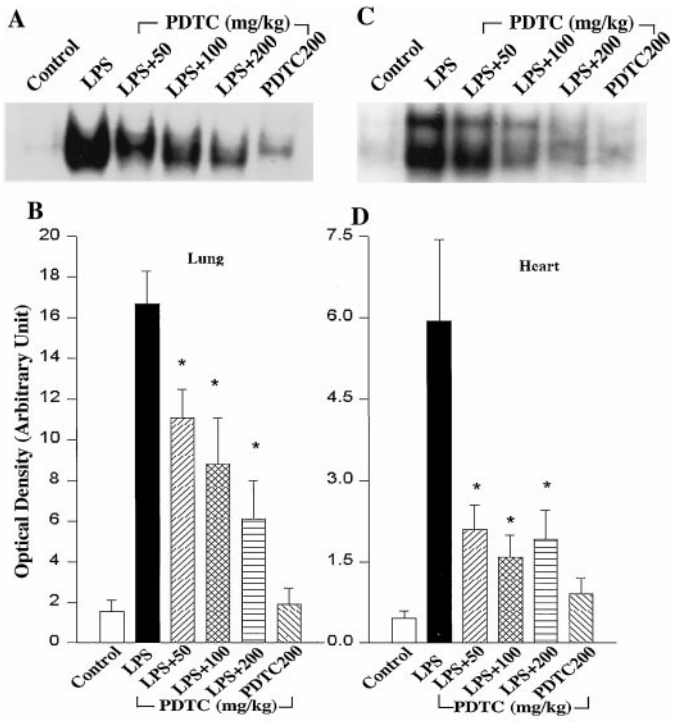

Fig. 1. PDTC inhibited LPS-induced NF-κB activation in lungs and heart. Tissues were isolated at 1 h after LPS. Nuclear protein was extracted, and EMSA was carried out as described in *Materials and Methods*. A, EMSA autoradiogram showing the inhibition by PDTC of LPS-induced NF-κB activation in the lungs. *B,* bar graph showing the mean band intensity of EMSA autoradiograph in the lungs of control, LPS alone, LPS plus 50, 100, or 200 mg/kg of PDTC, or PDTC (200 mg/kg) alone treated rats, as quantified using densitometry and expressed as an arbitrary unit. *$p < .05$, compared with LPS alone. Mean ± S.E.M. of four animals in each group. C, EMSA autoradiogram showing the inhibition by PDTC of LPS-induced NF-κB activation in the heart. D, bar graph showing the mean band intensity of EMSA autoradiograph in the hearts of control, LPS alone, LPS plus 50, 100, or 200 mg/kg of PDTC, or PDTC (200 mg/kg) alone treated rats, as quantified using densitometry and expressed as an arbitrary unit. *$p < .05$, compared with LPS alone. Mean ± S.E.M. of four animals in each group.

Measurement of Tissue Myeloperoxidase Activity. We used tissue myeloperoxidase (MPO) activity as an index of tissue neutrophil accumulation. To measure tissue MPO activity, frozen lungs, hearts, and livers were thawed and extracted for MPO, following the homogenization and sonication procedure as described previously (Krawisz et al.,1984). MPO activity in supernatant was measured and calculated from the absorbance (at 460 nm) changes resulting from decomposition of H_2O_2 in the presence of *o*-dianisidine (Krawisz et al.,1984).

Measurement of Microvascular Permeability. Microvascular endothelial permeability was assessed using the dual tracer methods, which has been demonstrated to accurately estimate the permeability-surface product for albumin (Graham and Evans, 1991). Animals were anesthetized with sodium pentobarbital (50 mg/kg, i.p.) and ventilated with rodent ventilator at a tidal volume of 1 ml/100 g of body weight and frequency of 60 breaths/min. Left carotid artery and right jugular vein were cannulated for monitoring of blood pressure and for the injection of LPS and tracers. After a 20-min equilibration period, LPS (8 mg/kg, i.v.) or PDTC (50, 100, or 200 mg/kg, i.p.) was injected. This was followed by an injection of ^{125}I-labeled human serum albumin (1 μCi in 0.2 ml saline) via jugular vein cannula. At 5 h after LPS, animals were heparinized, and 1 μCi of ^{131}I-labeled human serum albumin was injected (via jugular vein). Five minutes after [^{131}I]-labeled human serum albumin injection, 1 ml of blood was withdrawn, and lungs, hearts, and livers were collected after the animal was exsanguinated. Tissues were dissected into small pieces, blotted free of surface water and blood, and weighed. Plasma and tissue ^{125}I and ^{131}I activities (cpm) were counted using a gamma counter. Extravascular albumin accumulation was calculated from the ratio of tissue to plasma ^{125}I counting, with the intravascular albumin retention being corrected with the ratio of tissue to plasma [^{131}I] countings.

Statistical Analysis

CINC, ICAM-1, and GAPDH bands on Northern blot and NF-κB bands on EMSA autoradiograph were quantitated using a laser densitometry (Howtek, Hudson, NH) linked to a computer analysis system (PDI, Huntington Station, NY). The relative CINC and ICAM-1 RNA levels were expressed as a percentage of their corresponding GAPDH bands. Data are presented as means ± S.E.M. Statistical analysis of results was performed using Kruskal-Wallis Rank test, followed by Mann-Whitney *U* test for stepward comparison.

Results

PDTC Inhibits LPS-Induced NF-κ B Activation. We previously reported that challenge of rat with LPS caused a time-dependent NF-κB activation and that the NF-κB/DNA complex predominately consists of p50 and p65 subunits of NF-κB protein family in the lungs (Liu et al., 1997). Here, we used PDTC, an inhibitor of NF-κB activation in vitro and in

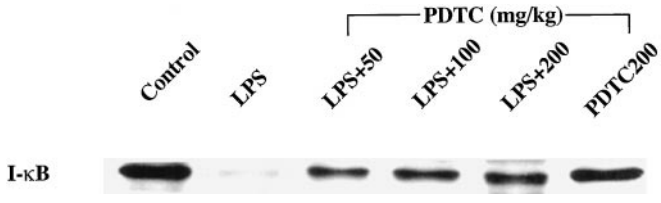

Fig. 2. Western blot photograph showing the prevention by PDTC of LPS-induced I-κBα degradation in the lungs. Lungs were isolated from control, LPS alone, LPS plus 50, 100, or 200 mg/kg PDTC and PDTC (200 mg/kg) alone treated rats at 1 h after LPS. Whole-cell protein was extracted, and Western blot was carried out as described in *Materials and Methods*. This is a representative of three separate experiments from three animals in each group.

vivo (Schreck et al., 1992; Ziegler-Heitbrock et al., 1992; Kawai et al., 1995; Liu et al., 1997), to study the role of NF-κB activation in mediating LPS-induced CINC and ICAM-1 expression and multiple organ injury. Figure 1, A and C, is an autoradiogram of EMSA showing LPS-induced NF-κB activation and its inhibition by PDTC. The NF-κB/DNA complex in the lung formed a single band (Fig. 1A) composed exclusively of p50 and p65 heterodimers, whereas NF-κB/DNA complex in the heart showed two bands (Fig. 1C). The lower band was composed of p50 and p65 heterodimer, whereas the upper band was composed of p65 homodimer, as demonstrated in our supershift assay. We quantitated these NF-κB bands using densitometry. Figure 1, B and D, is mean arbitrary units of these bands from lungs and hearts of four animals. The NF-κB/DNA binding activity was low in nuclear protein from control lungs and heart but was markedly increased in tissues from LPS-challenged rats. This LPS-induced NF-κB/DNA binding activity was inhibited by pretreatment with PDTC in a dose-related manner (Fig. 1).

PDTC Prevents LPS-Induced I-κB Degradation in Vivo. To investigate the possible mechanism of PDTC action in vivo, we treated animals with 50, 100, or 200 mg/kg PDTC for 1 h before challenge with LPS for 1 h and compared I-κBα protein abundance in lung homogenates of these rats to animals treated with saline (control) or LPS alone, using Western blot analysis. As shown in Fig. 2, LPS reduced the tissue I-κB protein content dramatically, whereas this was prevented by pretreatment with three doses of PDTC. The inhibition by PDTC of the LPS-induced I-κB degradation appears to be dose dependent (Fig. 2).

PDTC Inhibits LPS-Induced CINC and ICAM-1 mRNA Expression in Vivo. We studied the effects of inhibiting NF-κB activation with PDTC on LPS-induced CINC and ICAM-1 mRNA expression. We treated animals with 50, 100, or 200 mg/kg PDTC for 1 h before challenge with LPS for 4 h and compared CINC and ICAM-1 mRNA abundance in tissue homogenates of these rats to rats treated with saline (control) or LPS alone. As shown in Fig. 3, the 0.93-kb CINC mRNA transcript was absent or negligible in the control homogenates of both the lung and heart tissues (Fig. 3, A and C), whereas the 2.6-kb ICAM-1 mRNA transcript showed organ-dependent variation in its basal level (Fig. 4, A and C). ICAM-1 mRNA was negligible in control hearts (Fig. 4C) but was expressed in control lungs (Fig. 4A). The mRNA abundance of these two genes increased markedly after LPS challenge (Figs. 3A, 3C, 4A, and 4C). PDTC reduced the LPS-induced induction of these genes in a dose-related manner. PDTC alone did not affect their expression (Figs. 3 and 4). We quantified CINC, ICAM-1, and GAPDH band intensity using densitometry and normalized the CINC and ICAM-1 bands to their corresponding GAPDH bands. Neither LPS nor

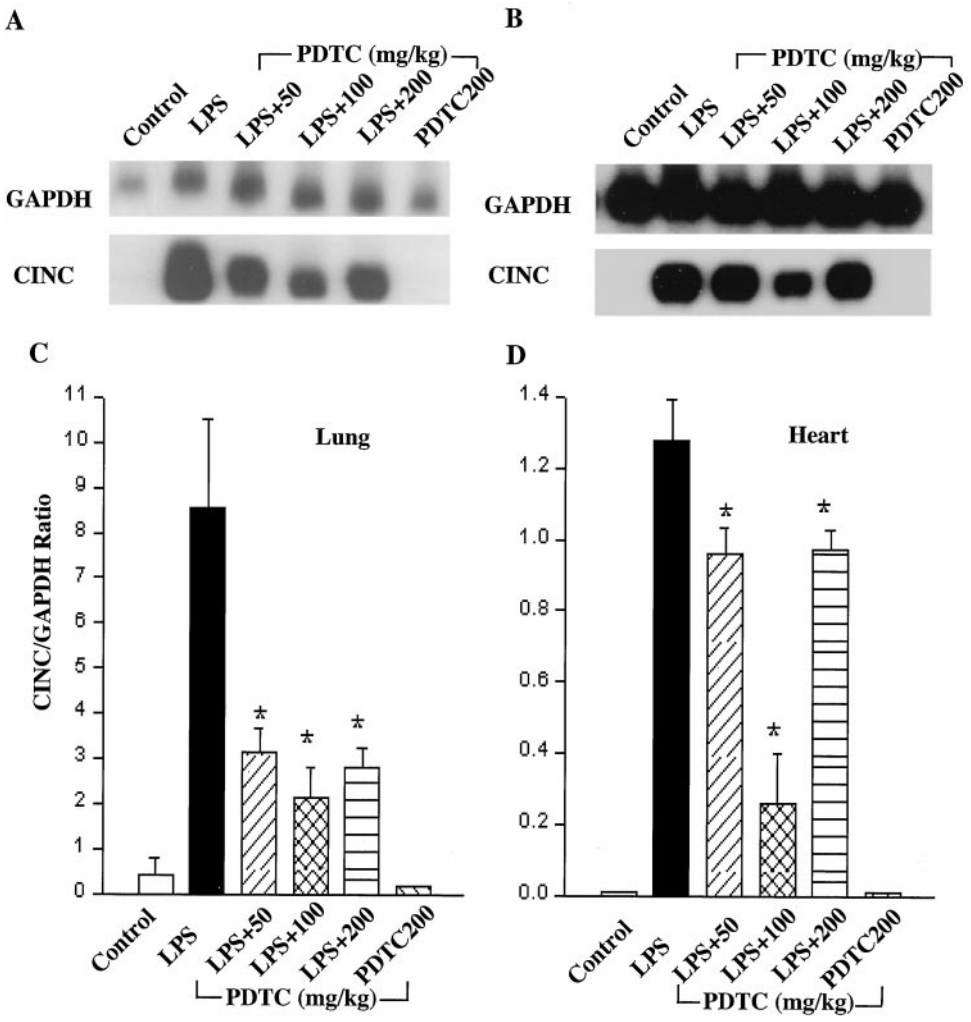

Fig. 3. PDTC inhibited LPS-induced CINC mRNA expression in lungs and heart. Tissues were isolated at 4 h after LPS. Northern blot analysis was carried out as described in *Materials and Methods*. A, Northern blot autoradiogram showing the inhibition by PDTC of CINC mRNA expression induced by LPS in the lung. GAPDH mRNA served as internal controls. B, relative CINC mRNA levels in the lungs of control, LPS alone, LPS plus 50, 100, or 200 mg/kg of PDTC, or PDTC (200 mg/kg) alone treated rats, as quantified by densitometry and expressed as CINC/GAPDH ratio (CINC/GAPDH absorbance ratio). *$p < .05$, compared with LPS alone. Mean ± S.E.M. of four animals. C, Northern blot autoradiogram showing the inhibition by PDTC of CINC mRNA expression induced by LPS in the heart. GAPDH mRNA serves as internal controls. D, relative CINC mRNA levels in the hearts of control, LPS alone, LPS plus 50, 100, or 200 mg/kg of PDTC, or PDTC alone (200 mg/kg) treated rats, as quantified by densitometry and expressed as CINC/GAPDH ratio. *$p < .05$, compared with LPS alone. Mean ± S.E.M. of four to six animals.

PDTC had a significant effect on the GAPDH mRNA transcription (Figs. 3A, 3C, 4A, and 4C). However, LPS increased the CINC/GAPDH and ICAM-1/GAPDH ratios markedly (Figs. 3B, 3D, 4B, and 4D). PDTC at concentrations of 50, 100, and 200 mg/kg, respectively, reduced LPS-induced CINC mRNA level by 63, 74, and 67% in the lung (Fig. 3B) and by 25, 79, and 24% in the heart (Fig. 3D). PDTC reduced LPS-induced ICAM-1 mRNA level by 63, 75, and 60% in the lung (Fig. 4B) and by 22, 43, and 34% in the heart (Fig. 4D) at the PDTC concentrations of 50, 100, and 200 mg/kg, respectively.

PDTC Inhibits LPS-Induced CINC and ICAM-1 Protein Expression. To address whether inhibition of CINC and ICAM-1 mRNA expression by PDTC resulted in inhibition of protein expression, we compared CINC and ICAM-1 protein levels in tissue homogenates of lungs, hearts, and livers from control rats; rats challenged with LPS for 4 h; rats pretreated with 50, 100, or 200 mg/kg PDTC for 1 h before challenge with LPS for 4 h; and rats treated with PDTC alone. We quantitated CINC and ICAM-1 protein level in tissue homogenates using Western blot and ELISA. Western blot analysis showed that the M_r 6,500 CINC and M_r 70,000 ICAM-1 proteins were detectable in the control homogenates but were markedly up-regulated by LPS challenge in all three organs (Figs. 5A, 5C, 5E, 6A, 6C, and 6E). Pretreatment with 50, 100, and 200 mg/kg of PDTC variably prevented the up-regulation of these two proteins (Figs. 5A, 5C, 5E, 6A, 6C, and 6E). A M_r 95,000 ICAM-1 protein was also detected in heart, which was up-regulated by LPS. This up-regulation was prevented by PDTC in a similar fashion as seen on the M_r 70,000 ICAM-1 protein (Fig. 6C). The 95-kD ICAM-1 protein band was not seen in lung and liver homogenates (Fig. 6, A and E), suggesting a differential glycosylation pattern in the myocardium.

ELISA results showed low CINC protein levels in control lungs and heart (Fig. 5, B and D), which increased by 3.1- and 6.1-fold in lungs and heart of LPS-challenged animals, respectively (Fig. 5, B and D). Pretreatment of LPS-challenged animals with 50, 100, and 200 mg/kg of PDTC reduced the LPS-induced elevation in tissue CINC content by 58, 60, and 42% in the lungs and by 67, 68, and 66% in the heart, respectively (Fig. 5, B and D). PDTC alone had no effect on CINC protein level in both organs (Fig. 5, B and D). Western blot showed a clear inhibition of LPS-induced CINC protein level in the liver (Fig. 5E). Therefore, we did not run CINC ELISA on liver protein.

Consistent with the mRNA data, ELISA results showed a variable level of ICAM-1 protein expression in control tissues. The basal ICAM-1 protein level was low in the heart, relatively high in the liver, and high in lungs (Fig. 6, D, F, and B). LPS challenge increased tissue ICAM-1 protein level by 1.6-, 2.0- and 3.4-fold in lungs, heart, and liver, respec-

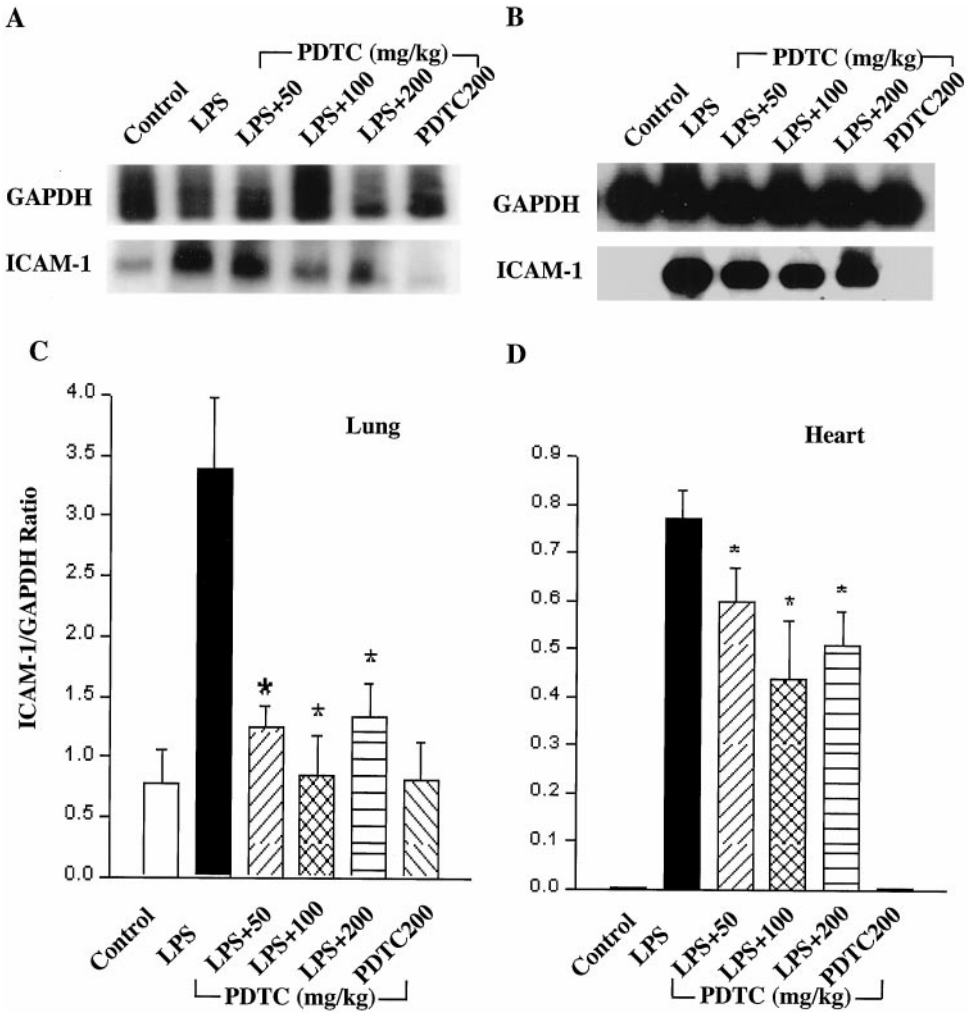

Fig. 4. PDTC inhibited LPS-induced ICAM-1 mRNA expression in lungs and heart. Tissues were isolated at 4 h after LPS. Northern blot analysis was carried out as described in *Materials and Methods*. A, Northern blot autoradiogram showing the inhibition by PDTC of ICAM-1 mRNA expression induced by LPS in the lungs. GAPDH mRNA serves as internal controls. B, relative ICAM-1 mRNA levels in the lungs of control, LPS alone, LPS plus 50, 100, or 200 mg/kg of PDTC, or PDTC (200 mg/kg) alone treated rats, as quantified by densitometry and expressed as ICAM-1/GAPDH ratio. $*p < .05$, compared with LPS alone. Mean ± S.E.M. of four animals. C, Northern blot autoradiogram showing the inhibition by PDTC of ICAM-1 mRNA expression induced by LPS in the heart. GAPDH mRNA serves as internal controls. D, relative ICAM-1 mRNA levels in the hearts of control, LPS alone, LPS plus 50, 100, or 200 mg/kg of PDTC, or PDTC (200 mg/kg) alone treated rats, as quantified by densitometry and expressed as ICAM-1/GAPDH ratio. $*p < .05$, compared with LPS alone. Mean ± S.E.M. of four to six animals.

tively (Fig. 6, B, D, and F). PDTC reduced the LPS-induced tissue ICAM-1 protein concentration by 16, 31, and 33% in the lung; 35, 38, and 42% in the heart; and 55, 62, and 68% in the liver at the PDTC concentration of 50, 100, and 200 mg/kg, respectively (Fig. 6, B, D, and F). PDTC alone had no effect on tissue ICAM-1 concentration in all three organs (Fig. 6, B, D, and F).

PDTC Reduces LPS-Induced Tissue MPO Activity. We studied the functional consequence of inhibiting NF-κB activation by PDTC on neutrophil influx into organs using MPO activity as an index of tissue neutrophil accumulation. As shown in Fig. 7, control tissues of all three organs had low MPO activity. The MPO activity increased markedly in all three organs 4 h after LPS challenge (Fig. 7). PDTC, at the concentration of 50, 100, and 200 mg/kg, respectively, reduced the LPS-induced tissue MPO activity by 51, 59, and 49% in the lungs; by 49, 56, and 49% in the heart; and by 41, 47, and 40% in the liver (Fig. 7). PDTC alone had no significant effect on tissue MPO activity in heart and liver but increased MPO activity in the lung (Fig. 7).

PDTC Reduces LPS-Induced Increase in Microvascular Permeability. We assessed the functional consequence of inhibiting NF-κB activation by PDTC on LPS-induced organ injury. We compared the microvascular endothelial permeability index in the lungs, heart, and liver of control, LPS alone, LPS plus various doses of PDTC, and PDTC alone treated animals. Challenge with LPS caused a 4.4-, 2.6- and 6.2-fold increase in the microvascular endothelial permeability index in lungs, heart, and liver, respectively (Fig. 8). Pretreatment of the LPS-challenged animals with 50, 100, and 200 mg/kg of PDTC reduced the LPS-induced elevation in permeability by 52, 53, and 47% in the lungs; by 41, 47, and 41% in the heart; and by 58, 61, and 56% in the liver (Fig. 8). The maximal inhibition of LPS-induced increase in microvascular permeability was observed at the PDTC concentration of 100 mg/kg in all three organs.

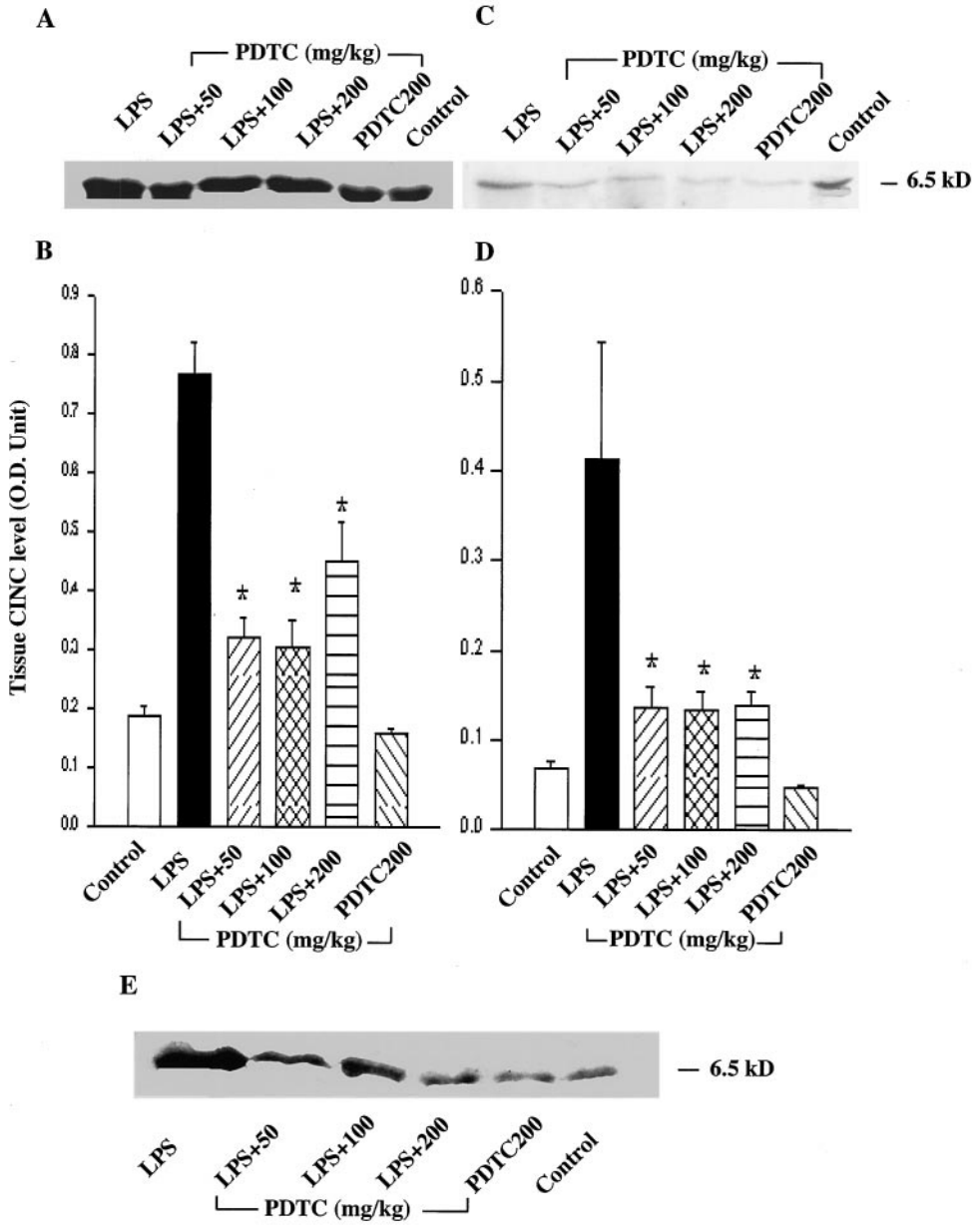

Fig. 5. PDTC inhibited LPS-induced CINC protein expression in lungs, heart, and liver. Tissues were isolated at 4 h after LPS. The cytosolic fraction of protein was extracted, analyzed using Western blot, and quantified for CINC level using ELISA. A, Western blot photograph showing the inhibition by PDTC of CINC protein expression induced by LPS in the lungs. B, CINC protein levels in the lungs of control, LPS alone, LPS plus 50, 100, or 200 mg/kg of PDTC, or PDTC (200 mg/kg) alone treated rats. $^*p < .05$, compared with LPS alone. Mean ± S.E.M. of four animals. C, Western blot photograph showing the inhibition by PDTC of CINC protein expression induced by LPS in the heart. D, CINC protein levels in the hearts of control, LPS alone, LPS plus 50, 100, or 200 mg/kg of PDTC, or PDTC (200 mg/kg) alone treated rats. $^*p < .05$, compared with LPS alone. Mean ± S.E.M. of four animals. E, Western blot photograph showing the inhibition by PDTC of CINC protein expression induced by LPS in the liver.

This was the same concentration at which PDTC maximally inhibited LPS-induced CINC and ICAM-1 mRNAs (Figs. 3B, 3D, 4B, and 4D), CINC protein expression (Fig. 5, B and D), and tissue MPO activities (Fig. 7) in these organs.

Discussion

The major focus of the present study was to determine the role of NF-κB activation in mediating LPS-induced multiple organ injury. We inhibited the activation of NF-κB using PDTC and addressed the effects of this inhibition on LPS-induced CINC and ICAM-1 mRNA, protein expression, tissue neutrophil sequestration, and the subsequent LPS-induced increase in microvascular permeability in multiple organs. We demonstrated that PDTC inhibited LPS-induced I-κBα degradation and the resultant NF-κB activation in vivo in a dose-related manner. Pretreatment of rats with PDTC, ranging from 50 to 200 mg/kg body weight, also inhibited LPS-induced CINC and ICAM-1 mRNA and CINC and ICAM-1 protein expression. We found that the reduced expression of CINC and ICAM-1 correlated with important functional consequences because PDTC also abrogated the LPS-induced tissue neutrophil sequestration and increase in microvascular endothelial permeability in multiple organs. Because PDTC is a potent inhibitor of NF-κB activation both in vitro and in vivo (Schreck et al., 1992; Ziegler-Heitbrock et al., 1992; Kawai et al., 1995; Liu et al., 1997), the inhibition by PDTC of NF-κB activation and the suppression of LPS-induced CINC and ICAM-1 expression induced by LPS suggest that NF-κB activation mediates in part the LPS-induced expression of these genes. The results indicate that NF-κB activation is a critical mechanism in LPS-induced neutrophil sequestration and multiple organ injury.

The role NF-κB in LPS- or cytokine-induced CINC and ICAM-1 gene expression has been defined in cultured cells (Jahnke and Johnson, 1994; Hou et al., 1994; van de Stolpe et al., 1994; Collins et al., 1995; Ledebur and Parks, 1995; Ohmori et al., 1995; Ohtsuka et al., 1996). LPS has also been shown to activate NF-κB and induce CINC and ICAM-1 mRNA expression in vivo (Manning et al., 1995; Blackwell et

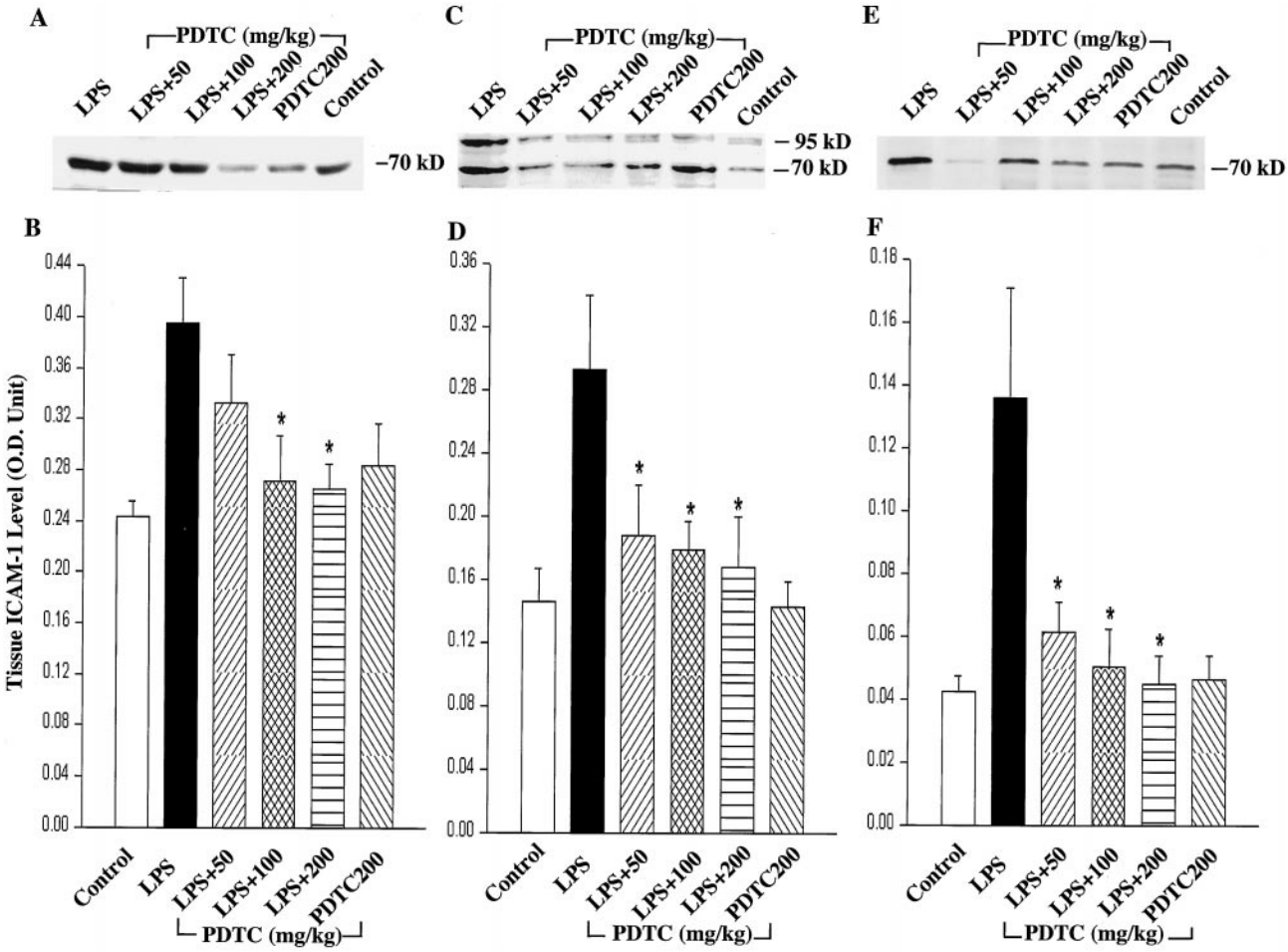

Fig. 6. PDTC inhibited LPS-induced ICAM-1 protein expression in lungs, heart, and liver. Tissues were isolated at 4 h after LPS. The membrane fraction of protein was extracted, analyzed using Western blot, and quantified for ICAM-1 level using ELISA. A, Western blot photograph showing the inhibition by PDTC of ICAM-1 protein expression induced by LPS in the lungs. B, ICAM-1 protein levels in the lungs of control, LPS alone, LPS plus 50, 100, or 200 mg/kg of PDTC, or PDTC (200 mg/kg) alone treated rats. *$p < .05$, compared with LPS alone. Mean ± S.E.M. of four animals. C, Western blot photograph showing the inhibition by PDTC of ICAM-1 protein expression induced by LPS in the heart. D, ICAM-1 protein levels in the hearts of control, LPS alone, LPS plus 50, 100, or 200 mg/kg of PDTC, or PDTC (200 mg/kg) alone treated rats. *$p < .05$, compared with LPS alone. Mean ± S.E.M. of four animals. E, Western blot photograph showing the inhibition by PDTC of ICAM-1 protein expression induced by LPS in the liver. F, ICAM-1 protein levels in the livers of control, LPS alone, LPS plus 50, 100, or 200 mg/kg of PDTC, or PDTC (200 mg/kg) alone treated rats. *$p < .05$, compared with LPS alone. Mean ± S.E.M. of four animals.

al., 1996). However, the in vivo function of NF-κB in mediating CINC and ICAM-1 gene and protein expression and its role in the development of organ injury has not been established. Our studies thus extend these previous observations by showing that inhibition of NF-κB activation in vivo suppresses LPS-induced CINC and ICAM-1 mRNA and protein expression, reduces neutrophil accumulation, and prevents the LPS-induced increase in microvascular endothelial permeability in multiple organs. Our study also establishes the in vivo linkage between NF-κB activation, adhesion molecule and chemokine expression, neutrophil sequestration, and the development of tissue injury.

We observed that PDTC had a greater inhibitory effect on LPS-induced NF-κB activation than on the expression of ICAM-1 gene in the heart, suggesting that additional transcription factors are also involved in LPS-induced ICAM-1 expression in vivo. This is consistent with results from cultured Mel Juso (human melanoma cell line) and Hep G2 cells (human liver heptoma cells), showing that tumor necrosis factor-α (TNF-α)-mediated induction of ICAM-1 promoter activity required the synergistic cooperation between NF-κB and C/EBP (nuclear factor for IL-6) (Jahnke and Johnson, 1994; Hou et al., 1994). Our results differ from the reported in vitro studies in human umbilical vein endothelial cells and

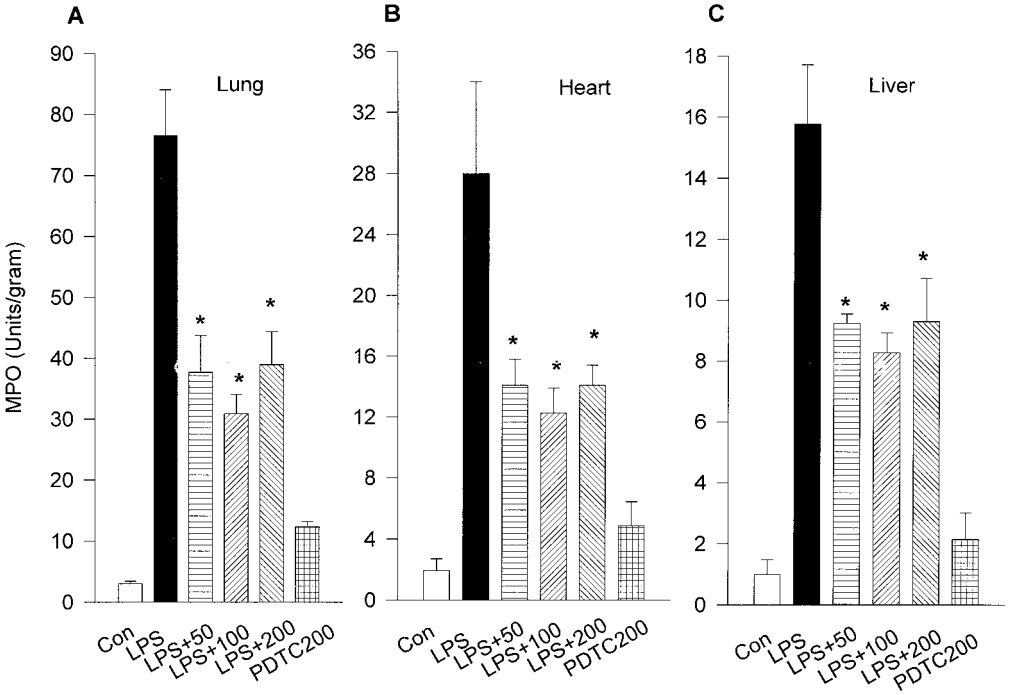

Fig. 7. PDTC inhibited LPS-induced tissue MPO activity in lungs (A), heart (B), and liver (C). Tissues were isolated 4 h after LPS. MPO was extracted and quantified as described in *Materials and Methods*. *$p < .05$, compared with LPS alone group. Mean ± S.E.M. of six animals.

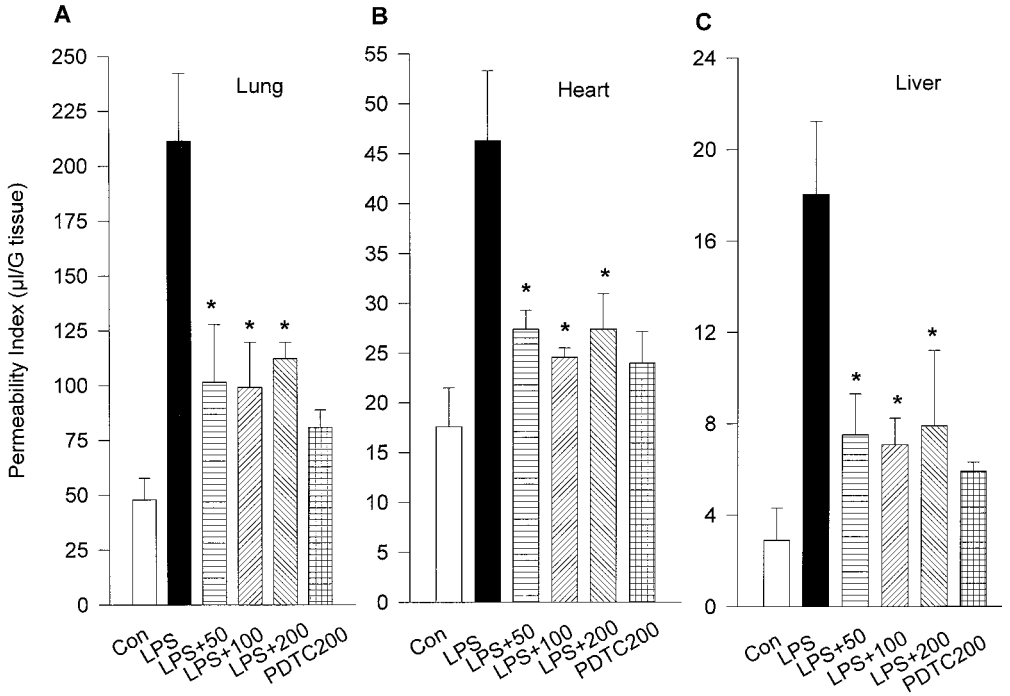

Fig. 8. PDTC inhibited LPS-induced increase in microvascular permeability in lungs (A), heart (B), and liver (C). Microvascular endothelial permeability was assessed at 5 h after LPS using dual tracers (^{125}I- and ^{131}I-labeled human serum albumin) method as described in *Materials and Methods*. *$p < .05$, compared with LPS alone group. Mean ± S.E.M. of five to seven animals.

U937 cells (human monocytic cell line) in which NF-κB alone was found to be sufficient for the induction of ICAM-1 promoter activity by in response to LPS or TNF-α (van de Stolpe et al., 1994; Ledebur and Parks, 1995).

Numerous in vitro studies have demonstrated PDTC to be a relatively selective inhibitor of NF-κB activation (Schreck et al., 1992; Ziegler-Heitbrock et al., 1993; Kawai et al., 1995; Munoz et al., 1996). It appears that PDTC is also an effective in vivo inhibitor of NF-κB activation (Liu et al., 1997). We observed that PDTC inhibited LPS-induced NF-κB activation in vivo but had no effect on the activation of other transcription factors, cAMP response element binding protein, Sp-1 (promoter-selective transcription factor), AP-1 (activating protein-1), and AP-2 (Liu et al., unpublished observation). Thus, PDTC is a useful pharmacological tool for the in vivo analysis of NF-κB activation and NF-κB-regulated gene expression.

One limitation to the use of PDTC is that a high dose of PDTC (200 mg/kg) has nonspecific effects. We observed that 200 mg/kg PDTC markedly augmented LPS-induced AP-1 activation and that this dose of PDTC alone activated AP-1 (Liu et al., unpublished observation). Because the promoter region of both ICAM-1 and CINC genes contain an AP-1 binding site (Collins et al., 1995; Ohmori et al., 1995) and activation of AP-1 is an important mechanism of LPS- or cytokine-induced expression of these genes (Collins et al., 1995), the inhibitory effect of PDTC mediated through NF-κB inhibition may be partially offset by its stimulation of AP-1 activation. This could explain why PDTC at 200 mg/kg was only partially effective as compared with 100 mg/kg of PDTC in preventing LPS-induced CINC and ICAM-1 mRNA and protein expression and LPS-induced MPO activity and the increase in microvascular permeability.

Nathens et al. (1997) have reported that PDTC failed to inhibit LPS-induced NF-κB activation in rats, in contrast to our in vivo finding and several in vitro studies (Schreck et al., 1992; Ziegler-Heitbrock et al., 1993; Kawai et al., 1995; Liu et al., 1997). Differences in cell types and duration of PDTC preincubation may explain this discrepancy. Nathens used nuclear protein from peritoneal macrophages of LPS-challenged rats for EMSA, whereas we used nuclear protein from whole lung and heart tissues; thus, it is possible that different cells can variably respond to PDTC. Nathens pretreated animals for 30 min, whereas we pretreated them for 60 min. Cell studies showed that PDTC exerted greater inhibitory effect on TNF-α- or PMA-induced NF-κB activation when the preincubation time was 1 h or longer compared with cells preincubated with PDTC for <1 h (Schreck et al., 1992; Ziegler-Heitbrock et al., 1993). We also observed that PDTC had little inhibitory effect on LPS-induced NF-κB activation when pretreatment time was <20 min, suggesting that a minimum preincubaion time is required for maximum PDTC inhibitory effect on NF-κB activation. Other factors such as time point at which EMSA was performed (3 h versus 1 h after LPS) and route of LPS administration (local versus systemic) could also contribute to this discrepancy.

The PDTC analog, dithiocarbamate, has been shown to inhibit HIV progression in patients (Reisinger et al., 1990), suggesting clinical usefulness of PDTC. However, there are limitations to the application of PDTC as a therapeutic NF-κB inhibitor: 1) the effective PDTC concentration range is narrow. According to our data, the minimal concentration of PDTC required to produce in vivo inhibition of NF-κB activation lies between 25 and 50 mg/kg, whereas at the PDTC concentration of 200 mg/kg animals showed toxic effects manifested as hypersalivation, excitability, and neuromuscular irritability; 2) PDTC has to be administered before the challenge, because PDTC was ineffective in inhibiting NF-κB activation when given concurrently with LPS (data not shown). A similar observation was reported in cell culture studies (Schreck et al., 1992; Ziegler-Heitbrock et al., 1993; Kawai et al., 1995). This probably reflects the time required for the accumulation of effective PDTC concentration in cytoplasm, where PDTC exerts its inhibitory action on NF-κB activation. The present results suggest the potential usefulness of a structurally modified PDTC with less toxic effects and greater efficacy.

The mechanisms of the action of PDTC remain obscure. PDTC is a well-known antioxidant. There is evidence supporting that PDTC suppresses NF-κB activation through its antioxidant property (Schreck et al., 1992; Satriano and Schlondorff, 1994), but contrary evidence also exists (Ziegler-Heitbrock et al., 1993; Satriano and Schlondorff, 1994; Brennan and O'Neill, 1995). We showed that PDTC prevented the LPS-induced I-κBα degradation, suggesting that PDTC acts upstream of I-κB degradation in the signaling cascade (perhaps at the level of I-κB phosphorylation or I-κB kinase activation) to prevent NF-κB activation in vivo.

We observed that the dose-response data in PDTC-mediated inhibition of ICAM-1 protein expression obtained by Western blot was not correlated with data obtained using ELISA (Fig. 6: A, C, and E versus B, D, and E). This inconsistency might be the result of an intrinsic variation. ICAM-1 protein, as determined in Western blot, is fully denatured by SDS treatment and boiling, whereas ICAM-1 protein, as determined in ELISA, may not be similarly denatured. The anti-rat ICAM-1 antibody used in these experiments was a blocking antibody. Because blocking antibody is designed to best recognize ICAM-1 protein in its natural conformation, it may have differential affinity to the determined ICAM-1 proteins. Thus, changes in ICAM-1 protein expression as determined by Western blot may not fully parallel measurement of ICAM-1 protein by ELISA.

In summary, we have shown that challenge of rats with LPS activated NF-κB and increased microvascular endothelial permeability in lungs, heart, and liver. Pretreatment of rats with PDTC inhibited the LPS-induced I-κBα degradation and resultant NF-κB activation in a dose-related manner and suppressed the LPS-induced CINC and ICAM-1 mRNA and protein expression in multiple organs. PDTC also reduced neutrophil accumulation in lungs, heart, and liver and attenuated the increase in microvascular endothelial permeability induced by LPS in these organs. These results suggest that NF-κB activation is a critical in vivo mechanism mediating LPS-induced multiple organ injury. Thus, inhibition of NF-κB activation may represent a novel therapeutic strategy for the treatment of sepsis-induced multiple organ injury.

Acknowledgment

We appreciate the technical support of Eun Mee Cheon.

References

Baeuerle PA and Henkel T (1994) Function and activation of NF-kappa B in the immune system. *Annu Rev Immunol* **12:**141–179.

Ben-Baruch A, Michiel DF and Oppenheim JJ (1995) Signals and receptors involved in recruitment of inflammatory cells. *J Biol Chem* **270:**11703–11706.
Blackwell TS, Blackwell TR, Holden EP, Christman BW and Christman JW (1996) In vivo antioxidant treatment suppresses nuclear factor-kappa B activation and neutrophilic lung inflammation. *J Immunol* **157:**1630–1637.
Bone RC (1991) The pathogenesis of sepsis. *Ann Intern Med* **115:**457–469.
Brennan P and O'Neill LA (1995) Effects of oxidants and antioxidants on nuclear factor kappa B activation in three different cell lines: evidence against a universal hypothesis involving oxygen radicals. *Biochim Biophys Acta* **1260:**167–175.
Brigham KL, Bowers R and Haynes J (1979) Increased sheep lung vascular permeability caused by *Escherichia coli* endotoxin. *Circ Res* **45:**292–297.
Carlos TM and Harlan JM (1994) Leukocyte-endothelial adhesion molecules. *Blood* **84:**2068–2101.
Chomczynski P and Sacchi N (1987) Single-step method of RNA isolation by acid guanidinium thiocyanate-phenol-chloroform extraction. *Anal Biochem* **162:**156–159.
Collins T, Read MA, Neish AS, Whitley MZ, Thanos D and Maniatis T (1995) Transcriptional regulation of endothelial cell adhesion molecules: NF-kappa B and cytokine-inducible enhancers. *FASEB J* **9:**899–909.
Frevert CW, Huang S, Danaee H, Paulauskis JD and Kobzik L (1995) Functional characterization of the rat chemokine KC and its importance in neutrophil recruitment in a rat model of pulmonary inflammation. *J Immunol* **154:**335–344.
Fort P, Marty L, Piechaczyk M, El Sabrouty S, Dani C, Jeanteur P and Blanchard JM (1985) Various rat adult tissues express only one major mRNA species from the glyceraldehyde-3-phosphate-dehydrogenase multigenic family. *Nucleic Acids Res* **13:**1431–1442.
Fowler AA, Hamman RF, Zerbe GO, Benson KN and Hyers TM (1985) Adult respiratory distress syndrome. Prognosis after onset. *Am Rev Respir Dis* **132:**472–478.
Graham MM and Evans ML (1991) A simple, dual tracer method for the measurement of transvascular flux of albumin into the lung. *Microvasc Res* **42:**266–279.
Hou J, Baichwal V and Cao Z (1994) Regulatory elements and transcription factors controlling basal and cytokine-induced expression of the gene encoding intercellular adhesion molecule 1. *Proc Natl Acad Sci USA* **91:**11641–11645.
Huang S, Paulauskis JD and Kobzik L (1992) Rat KC cDNA cloning and mRNA expression in lung macrophages and fibroblasts. *Biochem Biophys Res Commun* **184:**922–929.
Jahnke A and Johnson JP (1994) Synergistic activation of intercellular adhesion molecule 1 (ICAM-1) by TNF-α and IFN-γ is mediated by p65/p50 and p65/c-Rel and interferon-responsive factor Stat1 α (p91) that can be activated by both IFN-γ and IFN-α. *FEBS Lett* **354:**220–226.
Kawai M, Nishikomori R, Jung EY, Tai G, Yamanaka C, Mayumi M and Heike T (1995) Pyrrolidine dithiocarbamate inhibits intercellular adhesion molecule-1 biosynthesis induced by cytokines in human fibroblasts. *J Immunol* **154:**2333–2341.
Kita Y, Takashi T, Ligo Y, Tamatani T, Miyasaka M and Horiuchi T (1992) Sequence and expression of rat ICAM-1. *Biochim Biophys Acta* **1131:**108–110.
Koh Y, Hybertson BM, Jepson EK, Cho OJ and Repine JE (1995) Cytokine-induced neutrophil chemoattractant is necessary for interleukin-1-induced lung leak in rats. *J Appl Physiol* **79:**472–478.
Krawisz JE, Sharon P and Stenson WF (1984) Quantitative assay for acute intestinal inflammation based on myeloperoxidase activity. Assessment of inflammation in rat and hamster models. *Gastroenterology* **87:**1344–1350.
Ledebur HC and Parks TP (1995) Transcriptional regulation of the intercellular adhesion molecule-1 gene by inflammatory cytokines in human endothelial cells: Essential roles of a variant NF-kappa B site and p65 homodimers. *J Biol Chem* **270:**933–943.
Liu SF, Ye X and Malik AB (1997) In vivo inhibition of nuclear factor-kappa B activation prevents inducible nitric oxide synthase expression and systemic hypotension in a rat model of septic shock. *J Immunol* **159:**3976–3983.
Manning AM, Bell FP, Rosenbloom CL, Chosay JG, Simmons CA, Northrup JL, Shebuski RJ, Dunn CJ and Anderson DC (1995) NF-kappa B is activated during acute inflammation *in vivo* in association with elevated endothelial cell adhesion molecule gene expression and leukocyte recruitment. *J Inflamm* **45:**283–296.
Meyrick BO, Ryan US and Brigham KL (1986) Direct effects of *E. coli* endotoxin on structure and permeability of pulmonary endothelial monolayers and the endothelial layer of intimal explants. *Am J Pathol* **122:**140–151.
Mulligan MS, Schmid E, Beck-Schimmer B, Till GO, Friedl HP, Brauer RB, Hugli TE, Miyasaka M, Warner RL, Johnson KJ and Ward PA (1996) Requirement and role of C5a in acute lung inflammatory injury in rats. *J Clin Invest* **98:**503–512.
Munoz C, Pascual-Salcedo D, Castellanos MC, Alfranca A, Aragones J, Vara A, Redondo MJ and de Landazuri MO (1996) Pyrrolidine dithiocarbamate inhibits the production of interleukin-6, interleukin-8, and granulocyte-macrophage colony-stimulating factor by human endothelial cells in response to inflammatory mediators: modulation of NF-kappa B and AP-1 transcription factors activity. *Blood* **88:**3482–3490.
Nathens AB, Bitar R, Davreux C, Bujard M, Marshall JC, Dackiw AP, Watson RW and Rotstein OD (1997) Pyrrolidine dithiocarbamate attenuates endotoxin-induced acute lung injury. *Am J Respir Cell Mol Biol* **17:**608–616.
Ohmori Y, Fukumoto S and Hamilton TA (1995) Two structurally distinct kappa B sequence motifs cooperatively control LPS-induced KC gene transcription in mouse macrophages. *J Immunol* **155:**3593–3600.
Ohtsuka T, Kubota A, Hirano T, Watanabe K, Yoshida H, Tsurufuji M, Lizuka Y, Konishi K and Tsurufuji S (1996) Glucocorticoid-mediated gene suppression of rat cytokine-induced neutrophil chemoattractant CINC/gro, a member of the interleukin-8 family, through impairment of NF-κB activation. *J Biol Chem* **271:**1651–1659.
Parrillo JE (1995) Pathogenetic mechanisms of septic shock. *N Engl J Med* **328:**1471–1477.
Satriano J and Schlondorff D (1994) Activation and attenuation of transcription factor NF-κB in mouse glomerular mesangial cells in response to tumor necrosis factor-α, immunoglobulin G, and adenosine 3′:5′-cyclic monophosphate. Evidence for involvement of reactive oxygen species. *J Clin Invest* **94:**1629–1636.
Schreck R, Meier B, Mannel DN, Droge W and Baeuerle PA (1992) Dithiocarbamates as potent inhibitors of nuclear factor kB activation in intact cells. *J Exp Med* **175:**1181–1194.
Siebenlist U, Franzoso G and Brown K (1994) Structure, regulation and function of NF-κB. *Annu Rev Cell Biol* **10:**405–455.
Reisinger EC, Kern P, Ernst M, Bock P, Flad HD and Dietrich M (1990) Inhibition of HIV progression by dithiocarb. *German DTC Study Group Lancet* **335:**679–682.
Tate RM and Repine JE (1983) Neutrophils and the adult respiratory distress syndrome. *Am Rev Respir Dis* **128:**552–559.
van de Stolpe A, Caldenhoven E, Stade BG, Koenderman L, Raaijmakers JA, Johnson JP and van der Saag PT (1994) 12-O-Tetradecanoylphorbol-13-acetate- and tumor necrosis factor α-mediated induction of intercellular adhesion molecule-1 is inhibited by dexamethasone. Functional analysis of the human intercellular adhesion molecular-1 promoter. *J Biol Chem* **269:**6185–6192.
Ward PA (1996) Role of complement, chemokines, and regulatory cytokines in acute lung injury. *Ann NY Acad Sci* **796:**104–112.
Weiss SJ (1989) Tissue destruction by neutrophils. *N Engl J Med* **320:**365–376.
Wittwer AJ, Carr LS, Zagorski J, Dolecki GJ, Crippes BA and De Larco JE (1993) High-level expression of cytokine-induced neutrophil chemoattractant (CINC) by a metastatic rat cell line: Purification and production of blocking antibodies. *J Cell Physiol* **156:**421–427.
Ziegler-Heitbrock HW, Sternsdorf T, Liese J, Belohradsky B, Weber C, Wedel A, Schreck R, Bauerle P and Strobel M (1993) Pyrrolidine dithiocarbamate inhibits NF-κB mobilization and TNF production in human monocytes. *J Immunol* **51:**6986–6993.

Send reprint requests to: Dr. A. B. Malik, Department of Pharmacology (M/C 868), University of Illinois at Chicago, 835 South Wolcott Avenue, Chicago, IL 60612. E-mail: abmalik@uic.edu